Seventy Years of Radio Telescope Design and Construction

Jacob W. M. Baars[1] and Hans J. Kärcher[2]

[1]Max-Planck-Institut für Radioastronomie
Bonn, Germany
E-mail: jacobbaars@arcor.de

[2]MT Mechatronics
Mainz, Germany
E-mail: telescopemechanics@hjkaercher.de

Abstract

Radio radiation from the Milky Way was serendipitously discovered by Jansky in 1932. Reber used a home-built parabolic reflector to map the "radio sky" around 1940. Radio astronomy quickly developed after 1945, and the first large reflectors appeared in 1956-1961, operating at wavelengths of 20 cm and longer. A trend to shorter wavelengths and larger reflectors pushed structural design to include precision in addition to stiffness. A breakthrough was achieved in the mid-sixties by the concept of homologous deformation, and the use of advanced finite-element-analysis programs. The largest fully steerable radio reflectors of 100 m diameter can be used to a wavelength of less than 1 cm, while the most-precise reflectors of 10 m to 15 m diameter operate at 0.3 mm (1 THz).

We review the development of the design methods over time by example of selected radio telescopes where new design or material choices were made. These are the early telescopes in Jodrell Bank, Dwingeloo, and Parkes. The introduction of the homology principle, with its application to the Effelsberg telescope, opened the door to highly precise, large telescopes for mm-wavelengths. These culminated in the MRT (Millimeter Radio Telescope, Spain), LMT (Large Millimeter Telescope, Mexico) and ALMA (Atacama Large Millimeter Array, Chile). We conclude with a discussion of the design features of the Sardinia Radio Telescope (SRT).

1. Introduction

Astronomy is an observational science. The astronomer uses a telescope to collect the electromagnetic radiation that reaches the Earth from the "sky." In analyzing the received signal, he or she draws conclusions as to the physical circumstances of the celestial "transmitter," a star, galaxy, planet, or cloud of gas or dust. Differently from the experimental physicist, the astronomer cannot perform an experiment by influencing the processes in the object. For centuries, astronomy was limited to the use of the one-octave-wide spectral range of visible light at wavelengths from 380 to 700 nanometers.

By chance, K. G. Jansky [1], while working on short-wave communication at the Bell Telephone Laboratories, in 1932 discovered strong noise-like radiation at 20 MHz from the direction of the center of our Galaxy. This added the radio regime to the available spectral domain for astronomical research. Initially, only one person, an engineer and radio ham by the name of Grote Reber, followed up with constructing a 9.6 m-diameter parabolic reflector in his backyard, and systematically recording "cosmic static." With difficulty, he managed to publish his observations in the *Astrophysical Journal* [2], where it drew attention from several "real" astronomers and radar engineers. After the War, the latter turned their radar antennas into receiving systems for the study of cosmic radiation, in particular in England, Australia, and the USA. By the end of the 1940s, these activities were called *radio astronomy*, exercised by *radio astronomers*.

The observations were mainly performed at meter wavelengths with dipole arrays. The prediction by van de Hulst in 1944 [3] of a detectable spectral line of neutral atomic hydrogen at a wavelength of 21 cm pointed to the need for a reflector antenna of sufficient area and surface precision. In Europe, these were available in the form of the 7.5 m-diameter "Würzburg Riese" radar antennas, left behind by the German occupation. They were used in the Netherlands, England, and Scandinavia, and also in the USA. The Dutch antenna confirmed the neutral hydrogen line a few weeks after its initial detection [4, 5]. Several groups made daily observations of the sun. In Cambridge, England, two reflectors were connected as an interferometer to establish accurate celestial positions of the new "radio sources." In relation to optical telescopes, radio telescopes suffer from an abysmally poor angular resolution. An optical telescope of only 10 cm diameter provides an angular resolution of about one arcsecond, while the Würzburg antenna at 21 cm had a beamwidth

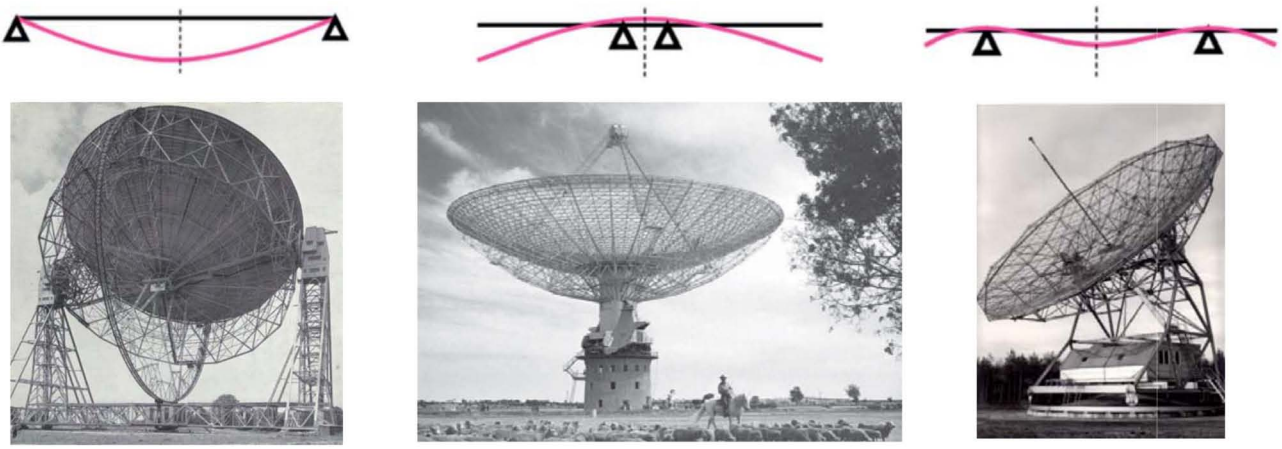

Figure 1. The (a) Jodrell Bank, (b) Parkes and (c) Dwingeloo telescopes (top to bottom), with their major deformation patterns illustrated above each telescope. The support scheme of the Dwingeloo telescope minimizes the overall sag.

of almost two degrees, which was a factor of 7000 poorer resolution. It also became clear that there were only a very few strong radio sources that can be properly studied by the existing instruments.

As a result, in the early fifties, several proposals were advanced for the construction of large paraboloidal reflector antennas. The existing groups also put strong efforts into the improvement of the sensitivity of the receivers. The choice of the paraboloid was obvious: it was a frequency-independent device with a single focal point, where the receiver could be located.

While selecting a large reflector was a simple matter, designing and constructing one was altogether another matter. The reflector needed to be directed to any point of the sky, and moreover, needed to be able to follow that point on its diurnal path. The reflector would thus have to be placed on a two-axis mount that provided precisely controlled angular movement about the axes. In addition, the parabolic shape of the reflector should be maintained with varying tilting angle to an accuracy of a small part of the observing wavelength. The important hydrogen line at 21 cm wavelength determined the minimum operational wavelength of the early large telescopes, requiring a surface precision of 1 cm rms error. The obvious candidates for designing a reflector radio telescope were people working on bridges, cranes, railroads, and airplanes. They could design large, stable structures, and handle survival requirements, such as storm loads. However, designing a large structure that moves in elevation angle and simultaneously rotates in azimuth, all the while maintaining reflector precision and pointing direction, forced them to think "outside the box."

The design features of the early radio telescopes have variously been applied and improved over time. Original design ideas have been introduced, and new materials have been incorporated in the development of ever-larger and more-precise instruments. In the following sections, we briefly summarize these developments by describing major radio telescopes built over the last 60 years.

2. The Early Radio Telescopes

The success of the detection of the hydrogen line inspired Jan Oort, at the Leiden Observatory, to propose a telescope of 25 m diameter. A young engineer, Ben Hooghoudt, worked with the company Werkspoor on the design. The telescope came into operation in Dwingeloo, the Netherlands, in 1956, and was for some time the largest fully steerable radio telescope in the world [6]. In Manchester, England, Bernard Lovell teamed up with a well-known bridge builder, Henry Charles Husband, to realize a gigantic reflector of 250-ft (76-m) diameter, which started work in 1957 [7]. Somewhat later, in Australia, Edward (Taffy) Bowen of CSIRO worked with Barnes Wallis, who had designed bombers for the Royal Air Force, on a 210-ft (64-m) telescope. Freeman Fox carried out the detailed design, and construction was finished in 1961 [8].

Quite different solutions for the support of the reflector by the mount were presented for the first large reflectors. The Jodrell Bank reflector is a closed, welded steel surface, and part of the load-bearing structure that is connected to the elevation bearings by a stiff outer hoop (Figure 1a). In the zenith position, this leads to a large central sag, as illustrated in Figure 1a. At intermediate elevation angles, an astigmatic deformation occurs. The "bicycle wheel" in the center does not carry loads, but stabilizes the structure against wind.

The Dwingeloo reflector is supported by a truss frame and connected to the elevation bearings about midway between center and rim (Figure 1c). This arrangement is optimal for the distribution of gravitational deformation and has been used for most large telescopes. The reflector surface is composed of triangular panels with a wire mesh of steel. These two telescopes have a *wheel-on-track* azimuth movement that has been selected for most telescopes from about 40 m diameter upwards.

The designers of the Parkes telescope took a completely different approach. A truss frame, resembling an aircraft hull, connected at the center to a stiff hub, supports the reflector. The deformation behavior is sketched in Figure 1b. Here, the maximum sag is at the reflector's rim, and a coma-type deformation occurs at intermediate elevation angles. The hub is connected to a compact elevation-azimuth mount placed on top of a concrete tower (Figure 1b). It reminds one of a cannon turret. This is often called a *turning head* mount. The reflector surface is a mesh over most of the area, with a small inner part of closed metal.

The early radio telescopes were essentially designed to provide sufficient stiffness against gravitational deformation as a function of elevation angle. The influence of moderate wind and possible temperature gradients on the reflector's precision and the pointing behavior could essentially be ignored for the envisaged wavelengths of observation.

All three antennas have undergone significant improvements over the years that upgraded their performance, in particular towards operation at shorter wavelengths. Jodrell Bank and Parkes are in full scientific use, while the Dwingeloo telescope is run by radio hams and astronomy amateurs, including an extensive program of outreach and education (camras.nl).

In the USA, several universities acquired telescopes between 15 m and 27 m in diameter in the later 1950s. The National Radio Astronomy Observatory was established in 1956, and operated a 26 m paraboloid since 1959; this was followed by a 92 m transit paraboloid in 1962 [9], and a high-precision 43 m telescope in 1965 [10], all located in Green Bank, West Virginia. Most of these telescopes had *equatorial (polar) mounts*, as did all optical telescopes at the time. Even the large 140-ft (43 m) telescope used a polar mount, which led to numerous problems in fabrication that could, at great cost and delay, be resolved. It is interesting to note that through state-of-art receivers and high-level operations support, this telescope became one of the most productive radio telescopes. An important factor here was the availability at short cm wavelengths, where it was preeminent for several years. A detailed story of the early NRAO telescopes was presented by Lockman et al. [11].

3. Homology Design and Its Derivatives

In the mid-sixties, astronomers were asking for larger reflectors that would perform well at short cm wavelengths. Efforts to use exiting telescopes in that wavelength region – in particular, early experience with the NRAO 140-ft telescope – showed serious performance deficiencies that would need to be addressed in next-generation telescopes. On the one hand, gravitational deformation as a function of elevation angle limited the optimal use of the telescope to a rather small angular range around the angle where the surface had been adjusted to its specified parabolic shape. Large-scale distortions, such as coma and astigmatism, caused significant loss of efficiency and reliability of observation. In addition, it became clear that variations and gradients in temperature of the support structure caused significant reflector deformation and additional pointing errors of the mount structure.

3.1 Summary of the Homology Principle

In a landmark paper, entitled "Design of Large Steerable Antennas," [12] Sebastian von Hoerner at the NRAO studied these limitations, and presented a new design method to significantly ameliorate their effects. He first derived the "basic natural limits" of a traditional telescope design, *gravitational*, *thermal*, *and stress*, and plotted these in a diagram of diameter as a function of the shortest operational wavelength, as shown in Figure 2. It was clear that the existing telescopes, indicated by the numbered dots, stayed well below the limits.

Von Hoerner then introduced a new structural-design method to overcome the gravitational limit, for which he coined the name *principle of homologous deformation*, briefly called *homology*. The idea is as simple as it is brilliant: *let the structure deform under gravitational load but in such a way that the surface retains a parabolic shape for all elevation angles, while allowing a change in focal length and axis direction.* The price to pay is the adjustment of the detector to the changing position of the focal point.

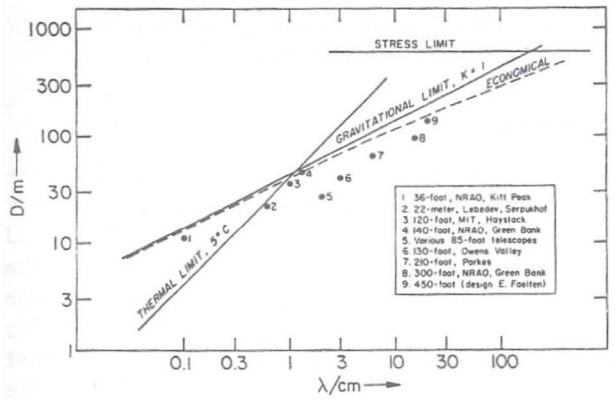

Figure 2. The natural limits to telescope size as a function of wavelength, with the values for a number of actual telescopes. All are more or less below the gravitational limit. The mm-telescope (no. 1) will be thermally limited during daytime (von Hoerner, 1967, [12]).

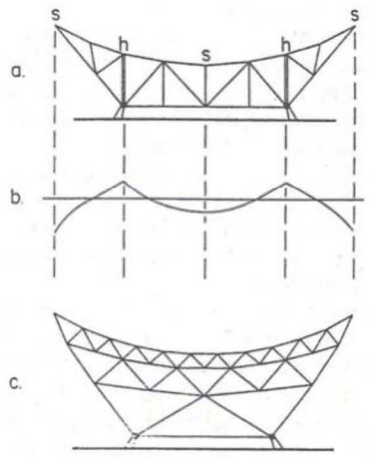

Figure 3. How an "equal softness" surface support is realized. The usual way (top) shows hard and soft points in the surface layer that lead to peaks and valleys in the surface, as depicted in the middle curve. By adding a few layers of trusses (bottom), the deformations are distributed, and the differences in deformations in the top layer become small [12].

A first goal was to create a reflector-support structure that would exhibit equal softness. As illustrated in Figure 3, this can be achieved by additional structural layers that smooth the deformation behavior of the surface.

To decouple the reflector structure from the "hard points" at the elevation bearings, which normally causes a strong "print-through" into the support structure, Von Hoerner used a basic octahedron between the reflector backup structure and the elevation bearings (Figure 4). This is called an *elevation cradle*. It transfers the loads of the reflector to the elevation bearings without causing print-through. The backup structure is connected to the cradle only at the lower central pivot by a conical circular set of struts that resemble an "inverted umbrella." The top cone of the octahedron functions as the quadripod support for the secondary reflector (or primary focus equipment) and penetrates the reflector structure without any contact, thereby avoiding the "point loads" on the structure and their unavoidable local deformation.

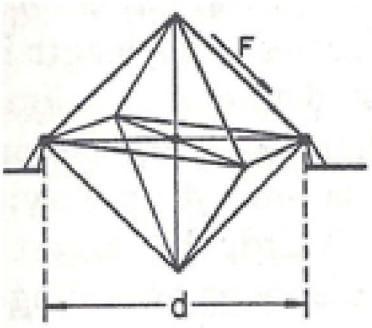

Figure 4a. Von Hoerner's original sketch of the octahedron concept for the elevation cradle.

3.2 Effelsberg 100-m Telescope

The homology principle was applied in the design of the Effelsberg 100-m telescope. For equal weights, the minimum wavelength of a homologous telescope can be more than an order-of-magnitude smaller than with a classical design based on stiffness. It is interesting to recollect here that once homology became known among telescope users, several older telescopes showed partially homologous behavior, which could be exploited by adjusting the detector to the "best focus" location depending on the elevation angle.

The consortium of Krupp and MAN designed the Effelsberg telescope in the late sixties. The sketch in Figure 5 shows the rigorous separation of the three major telescope sections: reflector with umbrella cone, octahedron elevation cradle with quadripod, and the wheel-on-track alidade. The picture in Figure 5 shows the highly symmetrical configuration of the reflector. It allowed the finite-element computer analysis of the structure despite the still-limited computer power at the time.

The basic ideas of von Hoerner were fully adopted, but the analysis and detailed design were done in house with available methods. The result was a telescope that surpassed its design specifications with a remarkably small total weight of 3150 tons, less than the Jodrell Bank 76 m telescope, and useable at a shortest wavelength of 7 mm. To illustrate the homologous behavior, in Figure 6 we show the position of the primary focus with respect to the structural prediction as a function of elevation angle [13].

Later, when comprehensive finite-element analysis programs became available, the design was run with these programs. The results showed deformation behavior very close to the original computations. In 2006, the 7.5 m

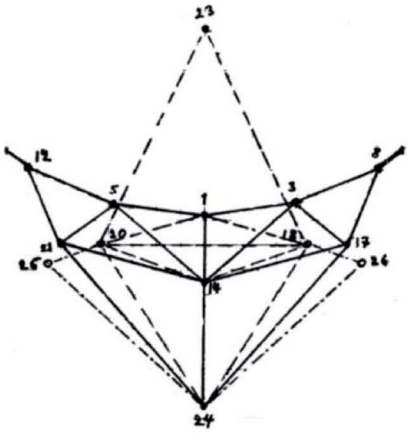

Figure 4b. The reflector backup structure, in solid lines, connected to the bottom of the cradle (dashed lines) by a number of struts (only three shown in solid lines), which form the "inverted umbrella" support.

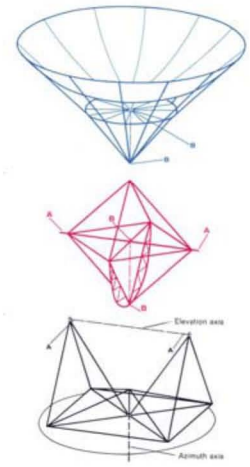

Figure 5a. The three main building blocks of the Effelsberg telescope: (blue) the reflector with umbrella cone; (red) the elevation cradle (octahedron) with elevation wheel; (black) the alidade with four bogies on a circular rail track.

diameter secondary reflector was replaced by an actively controllable surface. Depending on the computed large-scale deformation of the main surface as a function of the

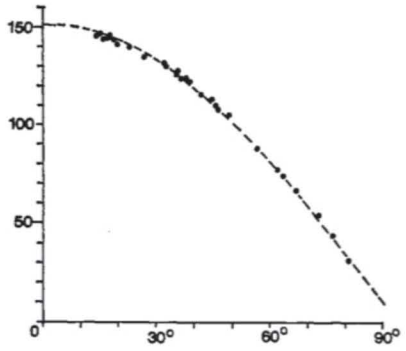

Radial movement of the prime focus (in millimeters) versus elevation (in degrees).

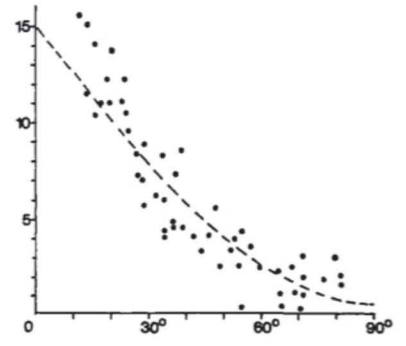

Axial movement of the prime focus (in millimeters) versus elevation (in degrees).

Figure 6. The radial (top) and axial (bottom) shifts of the primary focus in mm of the Effelsberg 100-m antenna as functions of the elevation angle. The dots are measurements; the line is the FEA computation. The larger spread in the lower plot was due to signal-to-noise restrictions during the measurements.

Figure 5b. A photograph of the 100-m telescope of the Max-Planck-Institut für Radioastronomie in Effelsberg, Germany. The telescope performs well at 7 mm wavelength, and acceptably at 3.5 mm (MPIfR).

elevation angle, the shape of the secondary was adjusted to obtain a flat phase function in the focal plane, providing a flat gain curve over the entire range of elevation angle and enabling observations at 3 mm wavelength.

3.3 Four-Point Support

The highly symmetrical layout of the inverted umbrella support for the Effelsberg reflector posed a serious problem of access to the Cassegrain focus behind the vertex with reflector diameters of less than about 50 m. For these antennas, a different solution for the connection between the homologous reflector's backup structure and

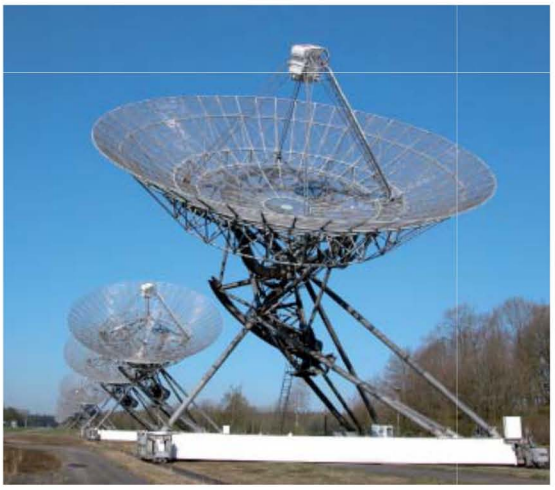

Figure 7. The Westerbork Synthesis Radio Telescope, with 14 polar-mounted 25-m antennas. Through the mesh surface, the declination cradle can be seen providing the four-point support for the reflector's structure and the quadripod. The circular gear-racks provide the movement in hour angle and declination. The two antennas in front can take any position on a 300 m-long rail track. The other fixed antennas are 144 m apart (ASTRON).

Figure 8. The 32-m Merlin telescope of the Jodrell Bank Observatory in Cambridge, UK. The reflector backup structure is connected to the ring girder at four positions 45° from the elevation bearings by flexures, visible in the middle of the detail picture (two nodes to the left of the red painted area) (H. Kärcher).

the elevation bearings needed to be found. A good solution was the application of a "cradle" that supported the BUS at four points, instead of at two, directly at the elevation bearings. The 25-m diameter polar-mounted antennas of the Westerbork Synthesis Radio Telescope (Figure 7), designed by Ben Hooghoudt, were the first to apply this solution in the mid-sixties [14]. This decreased the gravitational reflector deformation by an order of magnitude.

A further development was achieved by Hans Kärcher in the 32-m Merlin telescope in Cambridge (UK), by the introduction of a ring girder between the backup structure and the elevation bearings (Figure 8). The ring girder was equivalent to the "elevation cradle," and also carried the elevation-gear rim for the elevation drives. The four connecting points were arranged at the 45° symmetry lines. Shown in the small picture is this connection with flexures between the backup structure and the ring girder.

The principle of the layout and the calculated gravitational deformation of the reflector in zenith position are shown in Figure 9. Although the lower plot showed some print-through of the four support points, the overall deformation was an order-of-magnitude smaller than in the case of a two-point support directly at the elevation bearings, as shown in the upper plot. Clearly, the four-point support behaved in a reasonably homologous fashion, and it has been adapted for several telescopes with a diameter in the range of 15 m to 50 m. We shall meet variations of the four-point support in later sections.

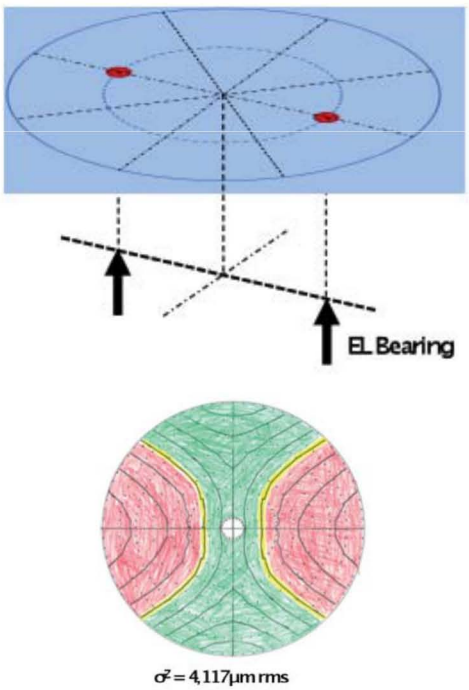

Figure 9a. The layout of the two-point support on the elevation bearings and the calculated gravitational deformation pattern in the zenith position, amounting to 4117 µm rms.

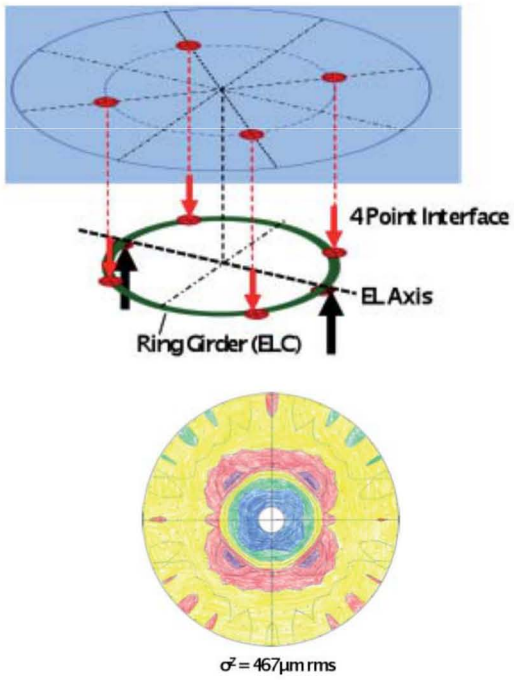

Figure 9b. The layout of the four-point ring-girder support of the reflector and the calculated gravitational deformation pattern in the zenith position, showing the decrease of deformation by an order of magnitude, to 467 µm.

3.4 The Green Bank Telescope (GBT)

Since its inception in 1957, the US National Radio Astronomy Observatory (NRAO) has taken up a number of projects to expand the available frequency range to observers. We mentioned above the 140-ft polar-mounted telescope that allowed observations at 2 cm wavelength. To offset the delay of the 140-ft in the early sixties, NRAO built a "quick and dirty" telescope in the form of a transit instrument of 300 ft (92 m) diameter. The telescope was restricted to a movement in elevation, and used the rotation of the Earth for the other coordinate. The telescope was designed and built in about one and one-half years, and started operation in September 1962 [9]. Its planned lifetime was five years. After a highly productive life of 26 years, material fatigue in an essential gusset plate caused the telescope to collapse on the evening of November 15, 1988. Its loss opened the way for the 100-m GBT (Green Bank Telescope).

Again, NRAO decided to develop uncharted territory by proposing a telescope of 100 m diameter in an *offset geometry* (Figure 10). Here, the reflector is a section of a paraboloid that lies outside the optical axis. The focal equipment, or the secondary reflector in a dual-reflector arrangement, together with its supporting structure, could be placed without causing any blocking of the main reflector. The most common prime-focus offset antenna is the ubiquitous personal satellite dish for the direct reception of satellite-borne TV transmissions. Such an optical arrangement exhibits superior electromagnetic performance in the form of higher aperture efficiency and a "clean" beam with low sidelobe structure. This was indeed the primary argument for the choice of the offset geometry, in that it would provide highly reliable observations of very weak and extended regions of radiation, both in our own Galaxy and external systems.

Figure 10. The Green Bank Telescope is an offset paraboloid of 100 m diameter. The reflector is actively adjusted to the correct shape by motorized adjusters on the basis of computed gravitational deformation. An overall surface error of 0.4 mm has been achieved (NSF/AUI/NRAO).

A goal of 0.4 mm rms precision of the reflector was set, to be competitive with the Effelsberg 100 m telescope. However, the offset antenna, with its highly asymmetrical geometry, had significant consequences for the structural design. In the design phase, it was realized that an active control of the surface and pointing of the telescope would be necessary. The project included a large effort in the realization of such a system. The construction of the telescope was started in 1991, and the telescope came into operation in 2002 [15]. We limit ourselves here to a few comments in the area of structural design, in particular in comparison to the Effelsberg telescope.

As in Effelsberg, the tipping structure of the Green Bank Telescope consists of a reflector backup structure and an elevation cradle. The topology of the backup truss is adapted to the shape of the surface panels. The elevation cradle carries the backup structure itself: the large arm for the support of the subreflector, and the gear rim for the elevation drive. The connection between the backup structure and the elevation cradle was concentrated to dedicated interface points in diameters about half of the overall reflector diameter, which resulted in a rather homologous deformation behavior. In contrast to the Effelsberg antenna (Figure 5), the alidade is designed as a very filigree truss system (Figure 10), thereby avoiding large box beams as used in Effelsberg. The total weight of the Green Bank Telescope is more than twice that of Effelsberg, which is partly due to the offset layout of the optics, but also to the different structural design, an approach probably driven by manufacturing and transportation aspects.

4. Millimeter-Wavelength Telescopes

4.1 Introduction

By the mid-sixties, the observations at short cm-wavelengths had shown the importance of extending the frequency range towards higher frequencies. This required the development of reflectors of very high precision, less than 100 μm for a wavelength of 2 mm. Simultaneously, it would be necessary to develop receivers for these frequencies. These would be based on Schottky diodes, which were in an early stage of development for frequencies of about 100 GHz.

As was the case with the 140-ft telescope, NRAO took the initiative to open this region for observation by building a dedicated *mm-telescope* of 11 m (36 ft) diameter, with a planned surface precision of 50 μm. The Earth's troposphere – in particular, water vapor – strongly absorbs radiation at millimeter wavelengths. For this reason, mm-telescopes must be located at high and dry sites, with a predominantly clear sky. For this reason, the telescope was located at 2000 m altitude on Kitt Peak observatory, near Tucson (Figure 11). The reflector is a single piece

Figure 11. The 36-ft (11 m) millimeter radio telescope of NRAO in its astrodome at an altitude of 2000 m at Kitt Peak Observatory near Tucson, Arizona. Operation started in 1968 (NSF/AUI/NRAO).

of aluminum, welded from a number of sheets and then machined in the paraboloidal shape on a large milling machine. The focal ratio is 0.8, unusually large for a radio reflector. The achieved surface precision is 100 μm, a factor two larger than specified. Particularly troublesome was the large thermal deformation between the aluminum dish and the steel backup structure. Good performance could only be obtained at night, in a state of thermal equilibrium. As the picture shows, the antenna was placed in an astrodome that was open towards the sky during observation.

Despite its shortcomings, the antenna was the largest available for wavelengths near 3 mm. It enabled the detection, in 1970, of the spectral line of interstellar carbon monoxide (CO) at 2.6 mm wavelength [16]. This caused a veritable run for observing time in the successful search for other molecules. By the mid-seventies, some 30 molecules had been identified by their mm-spectra. It was obvious that observations at mm-wavelengths were becoming highly significant for the development of astrophysics. Gordon told the story of this telescope in [17].

At the time, several proposals for a large mm-wavelength telescope were made in Japan, Germany, France, England, and the USA, ranging in size from 15 meters to 45 meters, with some suitable for wavelengths as short as 0.6 mm. To meet the performance requirements, it was necessary to improve on existing designs on essentially all fronts of antenna technology.

The major requirements could be summarized by two numbers:

1. Reflector surface precision not worse than about a twentieth of the shortest wavelength: hence, less than 100 μm rms;

2. Pointing and tracking precision of one-tenth of the beamwidth: of the order of one arcsecond.

These requirements had to be maintained under all operational conditions, including solar heating during the day, strong radiative cooling towards the clear sky at night, and generally relatively strong winds at the high mountain site.

This required significant improvement and new development in the hardware realization of the new instruments. For optimum – and normally, also most economic – performance of the telescope, the major contributions to the overall surface precision should roughly contribute equally. There are four major sources of error. If we assume that their contributions to the overall total precision can be added in a *root-sum-squared* fashion, it follows that each of them should not be larger than half the overall precision requirement. The four major factors are:

1. The individual panels composing the reflector surface. They need a fabrication precision of a few percent of the shortest wavelength. Table 1 summarizes the different types of panels and their accuracy.

Table 1. Typical design parameters of the most usual panel types (2016).

Type	Example	Maximum Size [m]	Typical Height [mm]	Typical Weight [kg/m^2]	Precision [μm rms]
Aluminum cassette	Effelsberg	2.5	200	20	>80
Aluminum or CFRP sandwich	MRT HHT	1.2	50	10	25 6
Machined aluminum	ALMA (NA)	0.8	50	10	<10
Electroformed nickel	ALMA (EU)	1.2	30	10	<10

2. The alignment of the panels to the desired reflector profile. In the early years, this was accomplished with geodetic methods, such as a theodolite and measuring tape. Photogrammetry has also been used [18], and has seen a recent revival with the newest digital cameras. In 1976, the method of *radio holography* was introduced [19], whereby a measurement of the antenna's radiation pattern (in amplitude and phase) provided the aperture field distribution after Fourier transformation. Deviations from constant phase in the aperture field are projected on the surface to deliver reflector profile deviations from the true paraboloid [20].

3. Gravitational deformation of the reflector's backup structure with elevation angle. Here, the designer meets the biggest challenge. The goal will normally be to realize homology as best as possible. As we have already seen above, practical requirements outside the direct structural design often pose certain limitations. In this review, we concentrate on these aspects of telescope design.

4. The influence of temperature variations and wind forces. With the growing size of the telescope and the simultaneous decrease of the shortest wavelength, the deformations caused by temperature variations in an open antenna structure became as significant as the remaining gravitational effects.

Temperature differences in the reflector structure decrease the surface precision, while differences in the support structure and mount – for instance, by one-sided solar illumination – cause pointing deviations that can easily be larger than the beamwidth [21].

Figure 12. The 30-m millimeter radio telescope (MRT) of IRAM at 2850 m altitude in the Sierra Nevada of southern Spain. Completely wrapped in thermal insulation and with active control of the temperature of the structure, it operates down to a wavelength of 0.8 mm (J. Baars, IRAM).

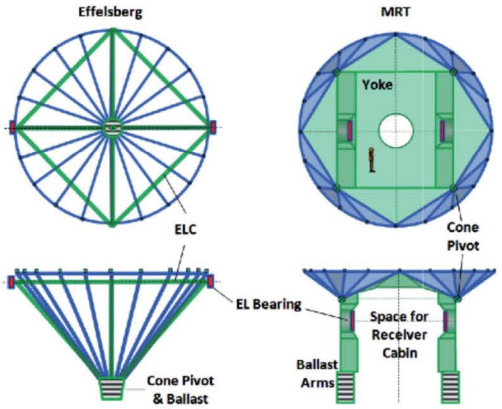

Figure 13. The Effelsberg umbrella (left) was changed in the MRT to a yoke, the corners of which function as the pivots for the box extension (blue) to a 14 m diameter plate for the support of the reflector backup structure (right).

Experiences at short wavelengths with the NRAO 140-ft and the Effelsberg telescopes had shown that the pointing accuracy and stability were as important as the reflector's surface precision. A 30-m diameter reflector has a half-power beamwidth (HPBW) of about 10 arcseconds at 1 mm wavelength. This requires a pointing precision of 1 arcsecond under operational circumstances. The designers thus had to give equal attention to the deformation of the reflector and to pointing deviations and fluctuations, all due to gravity, temperature differences, and wind. These were highlighted in the performance requirements for the Millimeter Radio Telescope (MRT), and were considered during the first conceptual design ideas for the 30-m millimeter telescope that was realized by the Max-Planck-Institut für Radioastronomie in Germany around 1980. The telescope was designed and constructed by a consortium of the companies Krupp and MAN, the same companies that had collaborated in the Effelsberg telescope project. Once operational, this instrument was handed over to the French-German Institute for Radio Astronomy in the Millimeter range (IRAM). The telescope is located at 2850 m altitude in southern Spain (Figure 12). We now describe its salient features.

4.2 The 30-m Millimeter Radio Telescope (MRT) of IRAM

As we already pointed out, the highly symmetrical umbrella support of the Effelsberg telescope is not feasible for smaller antennas because of the difficult access to the vertex area of the reflector. The solution for the interface from the backup structure to the elevation bearings for the MRT is sketched in Figure 14, with a comparison to the Effelsberg situation. In Effelsberg, the elevation cradle (in green lines) protruded into the umbrella cone of the backup structure (in blue lines) without contact except at the cone pivots. In the MRT, the cone pivot was split into

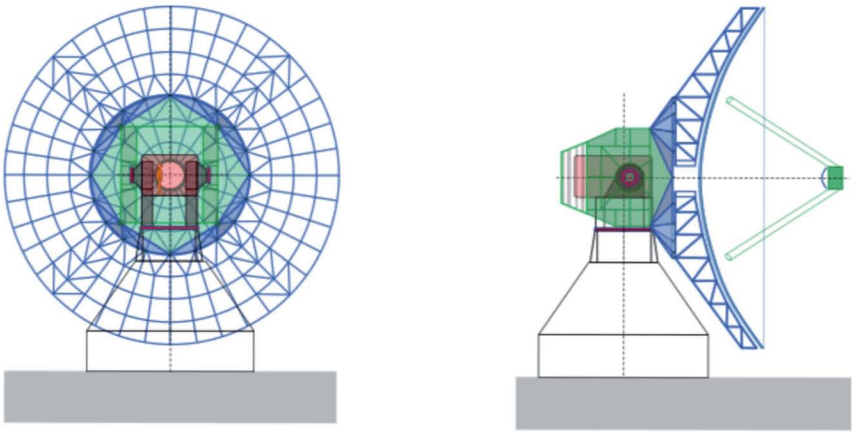

Figure 14. Rear and side views of the structural arrangement of the MRT.

four points at the outer corners of the yoke-type elevation cradle (right sketch), which left a free volume of space between the yoke (= ballast) arms. The deformation behavior of the MRT reflector is therefore equivalent to that of a four-point support.

From the four pivot points, the elevation structure was extended to a circular disc of 14 m diameter. The truss-frame backup structure of the reflector was supported at 20 points on the circumference of the disk, and a good homologous behavior was achieved [22]. Between the ballast arms there is space for a cabin with receiving equipment that is accessible during observations. As is visible in Figure 13, the ballast is somewhat offset from the symmetry line of the yoke arms. Through this feature, the unavoidable astigmatic deformation of a four-point support could be significantly reduced.

We noted earlier that one should not connect the quadripod for the support of the secondary reflector to the backup structure. This turned out to be impossible for the MRT, and the backup structure was adapted near the four corners to accommodate the quadripod. It is interesting to mention that the finite-element analysis of the combined backup structure and quadripod included the minimization of systematic pointing variation of the telescope as function of elevation angle. The pointing deviation between zenith and horizon is 80 arcseconds in the primary focus, and only 20 arcseconds in the Cassegrain focus. While this is a stable entity that can be calibrated, it decreases the time-variable wind pointing error by a similar fraction.

The structure is illustrated in Figure 14. We see the extra diagonals in the backup structure to accommodate the loads of the quadripod.

The rotation in azimuth was realized by a turning-head solution with a large slewing bearing of 5 m diameter on top of the concrete pedestal. This led to a compact overall layout of the telescope that leant itself to the application of thermal insulation.

After the gravitational deformations had been reduced to the required values, it became clear that thermal effects needed to be controlled to avoid deformation beyond the specifications. Computations showed that a uniformity of temperature of the major structural sections of about 1 K was required. This turned out to be very challenging.

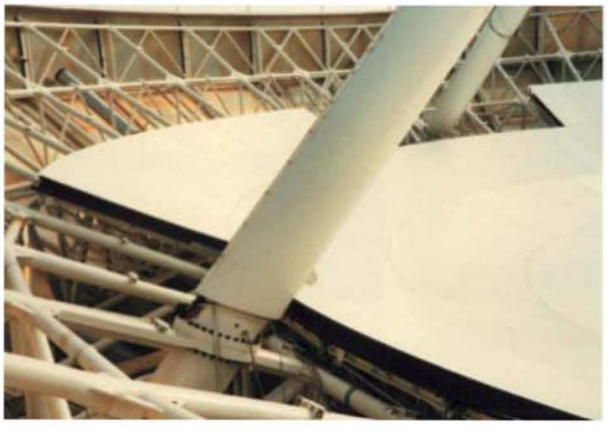

Figure 15a. Thermal insulation and a temperature controlled fluid are applied to control the temperature of the quadripod legs.

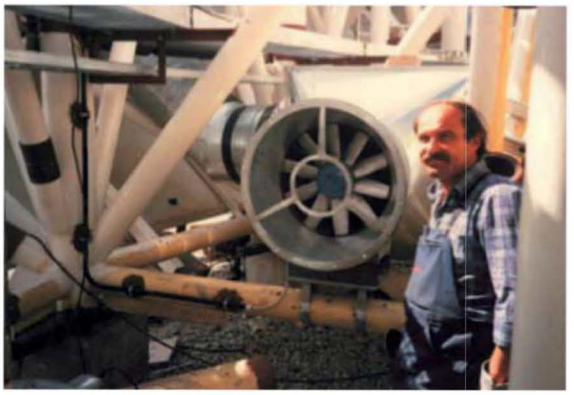

Figure 15b. One of the five ventilators that cause a circulating air movement with controlled temperature through the backup structure. This structure is covered on the outside by a cladding of thermal insulation panels, visible in the upper picture.

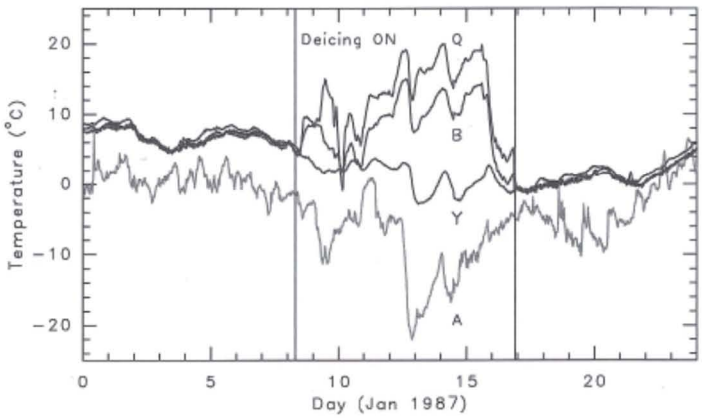

Figure 16. A plot of the temperatures over a full month of the ambient air (A), the yoke (Y), the backup structure (B), and the quadripod (Q). The left and right parts showed normal, satisfactory operation. In the center was a period of bad weather, during which the de-icing system was switched on and the control system was switched off. Note that the heating system kept the telescope just about above freezing.

Active control of the temperature and its homogeneity through the structure would clearly be unavoidable beyond whatever passive insulation one could install. As a result, a cladding of thermal insulation to smooth variations in ambient temperature and asymmetric solar illumination covers the entire telescope, apart from the surface, of course. The temperature of the reflector backup structure is kept at the temperature of the massive and slowly varying yoke structure by an actively temperature-controlled air-circulation system. The quadripod for the support of the secondary reflector was also temperature controlled. The pictures in Figure 15 give an impression of the air-circulation system and the insulation of the quadripod. The overall system realizes a uniform temperature through the telescope structure of about 1 K, and enables daytime observations under solar illumination with unimpaired performance.

The telescope at its high site is exposed to occasional strong snowfall and icing conditions. To avoid settling of ice on the antenna, the thermal insulation panels as well as the reflector surface can be heated from behind. Figure 16 presents an illustration of the performance of the thermal control system in varying conditions over a period of about three weeks in January 1987 [23]. Shown are the temperatures of the outside air (A), the heavy and compact yoke (Y) of the mount, the reflector backup structure (B), and the quadripod (Q) support of the secondary reflector. In the first eight days, we noted a close equality (to about 1 K) of the temperature of the three telescope sections, with a slow variation from day to day. The ambient temperature showed its diurnal variation and a slope towards a lower average value. Note that the telescope did not try to follow the ambient: rather, it kept the different sections at the same temperature. Of course, this avoided differential expansion within and between the sections. Halfway through day eight, the weather situation required the heating of the cladding – here, called "de-icing" – to be switched on. The bad weather continued until day 17. The leakage of the de-icing system into the structure inside disturbed the thermal control system beyond its capacity. It was actually switched off, and we saw a considerable heating of the backup and quadripod, but not in equal amounts, and a slow decrease of the yoke temperature. Once the de-icing was switched off and the control was system restarted, the telescope returned, in about a half day, to the usual uniformity and slow overall temperature variation that was mainly determined by the increase of the average daily ambient value.

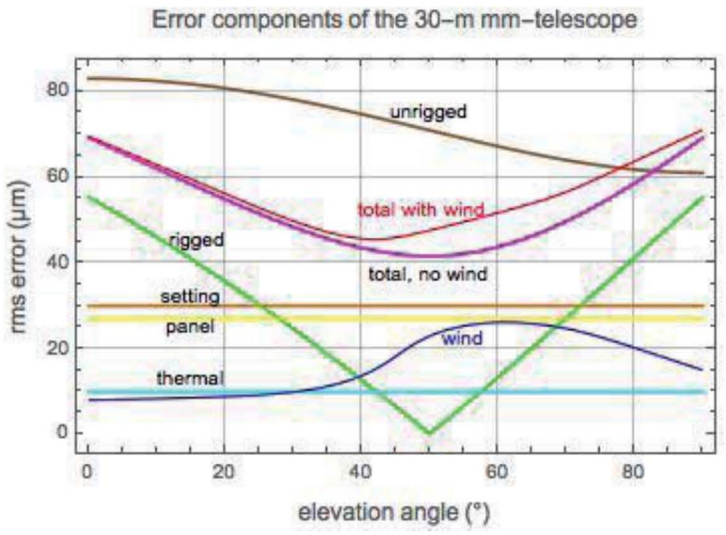

Figure 17. The error components of the MRT as functions of the elevation angle. The contributions from the panels (27 μm), the surface setting (30 μm), and thermal effects (10 μm) were constant. Wind deformation was computed from wind-tunnel measurements, while the gravitational deformation, shown in green, assumed a setting of the surface at 50° elevation. The "total" was the RSS average. The unrigged curve is the natural gravitational deformation.

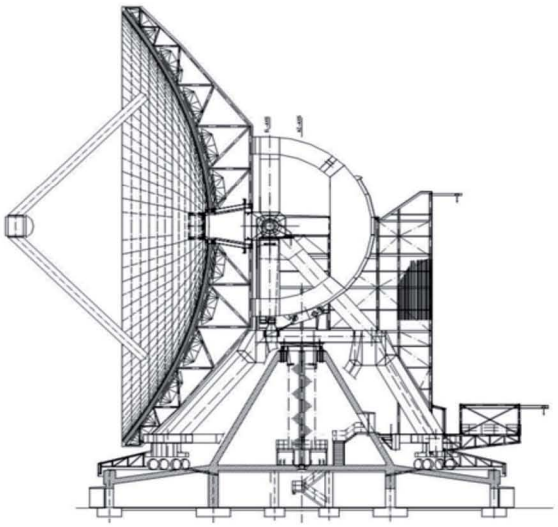

Figure 18a. A cross-section drawing of the Large Millimeter Telescope (LMT).

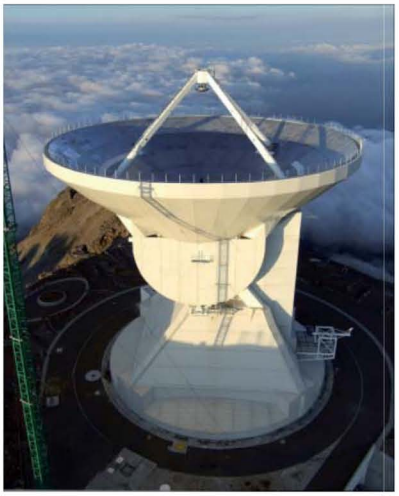

Figure 18b. A picture of the Large Millimeter Telescope (LMT) at 4600 m altitude on the Cerro la Negra in central Mexico (LMT).

Deformations of the reflector from wind forces are significantly less than the residual gravitational deformation and do not need to be corrected. Of more concern is the pointing fluctuation under wind. Here, the effects are minimized by an advanced servo-control system and corrections to the telescope axis direction measured by tilt meters.

To realize the goal of better than 100 μm surface precision, in addition to the structural and thermal performance, a method of measuring and setting the reflector surface to a higher precision was needed. The surface consists of about 200 surface-panel units, attached to the backup structure by adjustment screws that can be set with an accuracy of about 5 μm. After assembly, the position of the surface panels needed to be measured and set as well as possible to the prescribed paraboloid. At the start of the project, no measurement method with an accuracy of 50 μm was available. An in-house project using a modulated-laser distance-measurement device was started. However, as we mentioned in the introduction to the MRT description, the method of radio holography looked very promising, provided we could arrange for a strong signal source at a sufficiently short wavelength (of the order of 1 cm) and at a very large distance. Right at that time, an extremely strong maser source of water vapor at 22 GHz appeared in the Orion region. It was decided to also develop equipment and software to apply radio holography for the final setting of the reflector's surface. This was achieved in 1985 to a measurement accuracy of about 40 μm [24] and a reflector precision of 85 μm. Over time, the measurements have become more accurate, and control of the antenna has improved to a current surface quality of about 60 μm. The overall performance of the MRT reflector is summarized in Figure 17. The MRT is the most-productive telescope at short mm-wavelengths.

4.3 The 50-m Large Millimeter Telescope (LMT) in Mexico

Ten years after the start of the routine operation of the MRT, in 1985, the Mexican Instituto Nacional de Astrofísica, Óptica y Electrónica (INAOE) in the province of Puebla, and the Astronomy Department of the University of Massachusetts (UMass) in Amherst, presented a plan for the construction of a mm-telescope of 50 m diameter for operation to a shortest wavelength of 1 mm. Cerro la Negra, at 4600 m altitude in central Mexico, was selected as the site. The technical requirements for an instrument of this size and precision went considerably beyond those of the MRT, although a number of its design features could be transferred to the LMT. This was not too surprising, because the design of the LMT originated with the MAN Company that participated in the design and construction of the MRT.

There were two major differences with respect to the MRT:

1. The *turning head* mount was exchanged for a "*wheel-on-track*" configuration for the azimuth movement. Inside the alidade, a concrete tower allows the position of an elevated pintle bearing that takes the lateral loads from the wind. This provides a significant improvement in performance under strong winds over the standard wheel-on-track configuration, such as, for instance the Effelsberg telescope.

2. With a diameter of 50 m and the goal of a surface precision of 70 μm, even a fully homologous reflector could not be economically realized. The surface panel frames were therefore connected to the backup structure by motorized adjusters to obtain the required

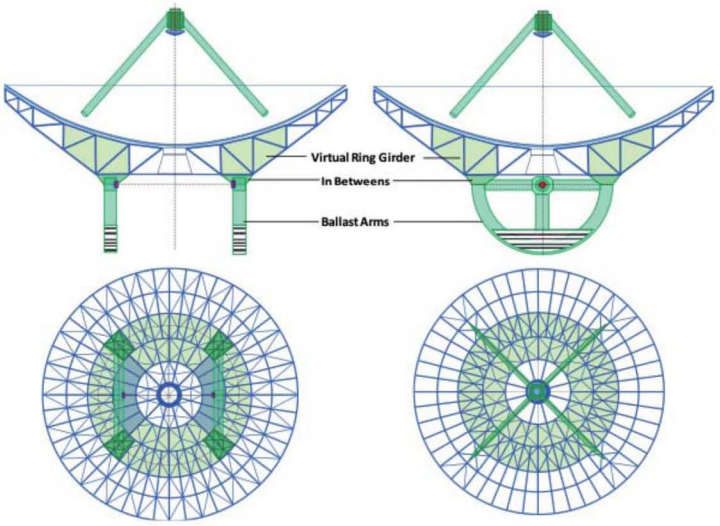

Figure 19. The design concept of the LMT reflector backup structure and its connection to the elevation structure at the corners of the ballast girders.

surface shape, with varying elevation angles based on finite-element computation or actual deformation measurements.

Of course, special measures had to be taken in the areas of thermal deformation and position control under wind, possibly well beyond the solutions installed on the MRT.

The telescope design followed the exposed concept, similar to that of the MRT. The backup structure and elevation cradle of the LMT were based on the same four-point concept as the MRT. The interface points of the ballast arms to the backup structure can be seen in the photo, sticking out from the cladding of the backup structure. The alidade of the LMT followed the wheel-on-track principle, because a sufficiently large slewing bearing, necessary for the size of the telescope, was not available at the time.

The telescope is protected on the outside by an insulated cladding and ventilators help to homogenize the temperature field inside the backup structure. However, there is no active temperature control as in the MRT. The cladding covers all structural components, including the reflector backup structure, the ballast arms and alidade, and also encloses a large two-story receiver cabin, with easy access via a staircase and elevator (visible on the right of the drawing and in the picture of Figure 18).

The reflector truss system is connected only in the 45° symmetry plane to the four endpoints of the ballast girders (Figure 19). A virtual ring girder inside the backup truss system, indicated in the figures by a light green shadowing, achieved the structural connection between the left and right ballast arm. It replaced the physical ring girder in the MERLIN design concept, respectively the "yoke disk" of the MRT de-sign. The ring girder functionality was achieved by the diagonals in both the upper and lower chords of ring 2 and 3 of the truss system, closing the truss topology of these rings also in regard to torsional loads.

The gravity deformations show some remaining print-through of the ballast arms. The rms deformation is about 300 μm in zenith position and about 400 μm in horizon position. This is some 10 times more than allowed for in the specified overall reflector precision of 70 μm rms. As noted, the design approach to the LMT was based from the beginning on the use of an *active surface*. The reflector panels are equipped with actuators for the open-loop correction of the gravity deformations via look-up tables obtained from the finite-element analysis. The active

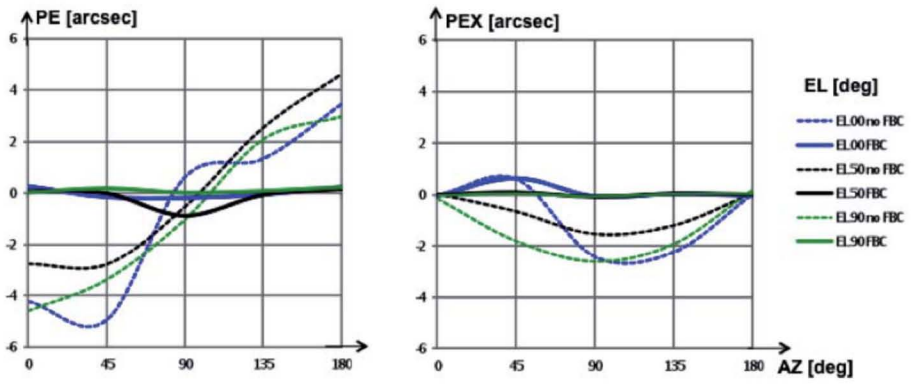

Figure 20. A comparison of the computed pointing errors of the LMTQ in elevation (PE) and cross elevation (PEX) for a 10 m/s wind speed. The dashed lines show the errors without active control, and the full lines show the errors with flexible body control (FBC).

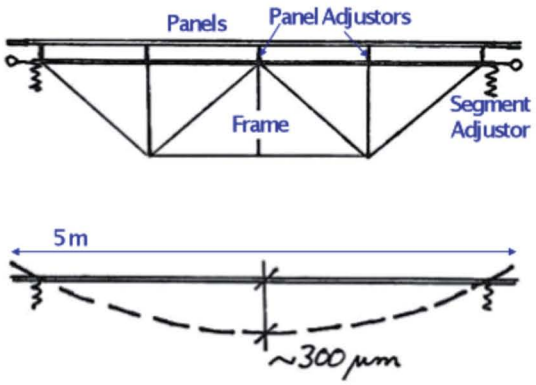

Figure 21a. A sketch of a 5 m wide "stiff" subframe and the sag of the surface (dashed line) by 300 µm.

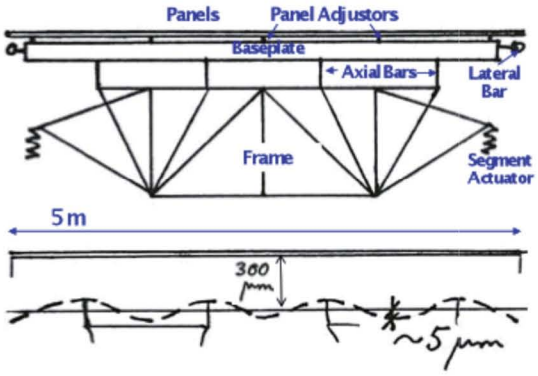

Figure 21b. A sketch of the same subframe as in Figure 21a, but isostatically supported at 8 points. The overall sag of the surface was still 300 µm, but the deviations of the theoretical surface were only of the order of 5 µm rms.

surface can also be used for correction of temperature-induced deformations. These are based on temperature measurements of the backup structure and a *thermal deformation model* for the calculation of the corrections. The active correction of wind-induced deformations would be much more complicated. However, the LMT backup structure is so stiff that the wind-induced deformations are just within the limits of the overall specification.

A more serious requirement is the stability of pointing under the influence of wind. The blind pointing specification of the LMT was of the order of 1 arcsecond under operational wind conditions of up to 12 m/s. Finite-element calculations, aided by results from wind-tunnel test data of the MRT, showed that the pointing errors would be up to 6 arcseconds. These data are shown in Figure 20 as dashed lines for the pointing error in elevation (PE) and cross-elevation (PEX) as functions of the attack angle (AZ) of the wind, and for three values of the elevation angle of the reflector.

The remedy is again the application of active compensation: this time, not at the surface, but at the drives of the main axes. Inclinometers were placed on the alidade in the vicinity of the elevation bearings. They measure the wind-induced deformations of the alidade, and these data are used for the calculation of the pointing variations and related corrections via the main-axes' drives. The full lines in Figure 20 show the simulated improvement obtained compared to the uncorrected error shown in dashed lines. Similarly feeding the data of a set of temperature sensors throughout the alidade and elevation structure to the finite element model yields a thermal-deformation pattern from which pointing corrections can be derived. These correction methods are called *flexible body compensation* (FBC). They are used in some form in most of the recent radio telescopes, such as, for instance, ALMA. Kärcher [25] presented the theoretical background, while Greve et al. [26] discussed results of flexible body compensation at the MRT.

Finally, we address the reflector surface. The precision of the LMT panels has to be in the range of 25 µm rms to fit into the overall surface-error budget of 70 µm rms. The available manufacturing processes limit the size of the panels of this surface accuracy to less than 1 m (Table 1). Similarly to the MRT, the LMT therefore used a sub-frame concept for the reflector surface that decouples the sizing of the panels from the spacing of the truss system for the backup structure. The spacing of the backup truss was chosen from the beginning to be about 5 m, between which the sub-frames had to span (Figure 21). The internal sag of a 5 m large sub-frame would be in the range of 300 µm (Figure 21a),

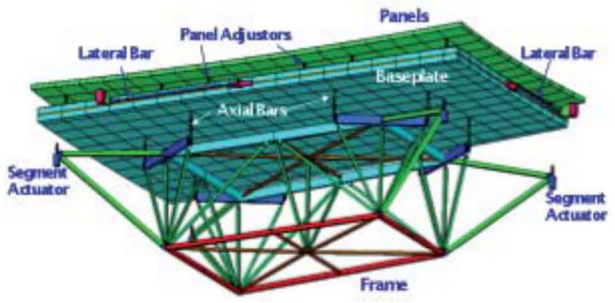

Figure 22a. A rendering of the finite-element model of the panel segment with panel, base plate, and isostatic support frame.

Figure 22b. A rear view of a panel unit installed in the backup structure of the LMT. The segments of about 5 m size are supported at their corners on the backup structure by motorized adjusters.

which was far above the overall accuracy requirement. The sub-frames were therefore following the *isostatic support* principle used for the mirrors of optical telescopes. The isostatic features achieved that the internal deformations of the subframes were inside the requirements, whereas the overall sag was still in the same range as the "simple" frames (Figure 21b). Finite-element analysis showed that the precision under gravity load could be improved by an order of magnitude.

Figure 22 shows a rendering of the finite-element model of the final design, and a view of the frame in the main truss structure. The isostatic subframes make the overall reflector system much more complex, and are only necessary for telescopes with accuracy requirements below 100 μm rms.

The construction of the LMT is expected to be completed by the end of 2017. The project has suffered long delays for a number of reasons, such as problems in the fabrication of surface panels and subreflector, management errors, and cost overruns. In June 2011, the reflector surface up to 32 m diameter had been installed and adjusted by holography, and the basic axis-control system was operational. A successful "first light" observation was made at 3.3 mm wavelength. Over the last three years, time has been devoted to observations at 3 mm and 1.3 mm, including successful participation in a few millimeter-VLBI observations.

In the meantime, the panels for the outer two rings have been delivered, and the installation is close to being completed. If the original specification can be met, the LMT/GTM will be a formidable addition to the available worldwide capacity for observations at short millimeter wavelengths.

Figure 23. Two sub-millimeter telescopes at 4000 m altitude on Mauna Kea, Hawaii. (a) The Caltech telescope, with a diameter of 10.4 m, operating at a shortest wavelength of 350 μm (S. Golwala, Caltech). (b) The JCMT with a diameter of 15 m, normally protected by a transparent skin covering the enclosure opening. Observations are made at wavelengths between 0.4 mm and 1.4 mm (Phillips, JCMT, Hawaii).

5. Sub-Millimeter-Wavelength Telescopes

5.1 Introduction

The richness of the "sky" at wavelengths from 1.2 mm to 7 mm, opened by the new mm-telescopes, inspired astronomers to propose telescopes useable up to about 1 THz (0.3 mm wavelength). At the highest and driest places on Earth, notably Hawaii, Northern Chile and the South Pole, the reduced atmospheric absorption allows observations at 1 THz under good weather conditions. These sub-millimeter telescopes need a surface precision of 20 μm, and a pointing quality of better than 1 arcsec. Preliminary studies in the mid-eighties indicated that the size of the reflector would be limited to 10-15 m in order to be economically viable. While at this relatively small size, gravitational deformation appeared to be controllable to values around 10 μm rms, the greatest problem arose in the reduction of thermal deformations. With standard materials like steel and aluminum, temperature gradients would need to be limited to a few tenths of a degree Celsius.

The first dedicated sub-mm telescope was designed and built by Robert Leighton at Caltech in the early eighties [27]. It had a diameter of 10.4 m, with an aluminum honeycomb reflector and a backup structure from steel. All members of the backup structure were rods of equal thickness and precise length. The structure was homologous, and the uniformity of the backup structure significantly reduced the effects of temperature change. Some active control of the surface was realized by differential heating of the 15 cm-long panel support rods. Located at 4150 m altitude on Mauna Kea, Hawaii (Figure 23a) since 1986, it was used at frequencies up to 800 GHz, until it was decommissioned in 2015. Four identical antennas of somewhat lower precision constituted the Caltech mm-array in Owens Valley, California [28].

Also on Mauna Kea and at about the same time, the British-Dutch-Canadian *James Clerk Maxwell Telescope* (JCMT) came into operation (Figure 23b). Like the Caltech

Table 2. The specified and achieved performance (in μm) for the Heinrich Hertz Telescope (HHT).

Error component	Specification	Achieved
Homology imperfection, assembly	7	<3
Space-frame residual deformation	7	<6
Panel fabrication	7	6
Panel residual deformation	7	<5
rss of structural/fabrication error	14	10
Reflector setting allowance	10	7
Overall rss error (μm)	17	12

telescope, a protective co-rotating dome surrounds the JCMT. However, in this case a fabric skin that keeps the wind out and lets the mm-radiation through normally covers the opening. The reflector has a diameter of 15 m. Aluminum honeycomb panels are supported by a steel backup structure through motorized adjusters. A detailed study was made of the thermal aspects [29], but control of thermal effects was difficult, in reality. The skin needed to be closed under most circumstances, and operation was limited to nighttime, enabling observations up to 700 GHz. The East Asian Observatory now operates the telescope.

5.2 The Sub-Millimeter Heinrich Hertz Telescope (SMT/HHT)

Clearly, the ever-changing thermal environment of the telescope posed the most serious limitation on achieving the required precision for operation in the sub-mm wavelength range. One really needed a structural material with an order-of-magnitude smaller thermal expansion, and strength comparable to steel or aluminum. A solution was offered by the composite carbon-fiber-reinforced plastic (CFRP) material that was already widely in use for space-born applications. By the mid-eighties, its widening application in commercial products lowered the price to a level where one could envisage its application in radio-telescope structures. Carbon-fiber-reinforced plastic had already been used for the surface panels of millimeter telescopes such as the 45-m telescope in Nobeyama [30], Japan, and the 15-m antennas of the IRAM interferometer in France [31].

Figure 24. The HHT sub-millimeter telescope in the opened enclosure at 3200 m altitude on Mt. Graham, Arizona. The truss frame backup structure (black) consists of carbon-fiber-reinforced plastic struts connected to invar steel nodes. The connection to the steel elevation structure (white) is made by 20 flexures of steel. These effectively absorb the difference in thermal expansion between backup and mount without introducing deformation into the backup structure (J. Baars, SMT Observatory).

The MPIfR, together with German industry, started a project for a sub-mm telescope that would have a backup structure of carbon-fiber-reinforced plastic supporting carbon-fiber-reinforced plastic panels. This essentially removed thermal effects from the list of major concerns. In collaboration with Steward Observatory of the University of Arizona in Tucson, a sub-millimeter telescope (SMT) of 10 m diameter was realized at 3200 m altitude in southern Arizona. It was baptized the Heinrich Hertz Telescope (HHT), but this name has been replaced by the original acronym SMT, since the Steward Observatory is the sole operator.

The upper part of the HHT is shown in Figure 24. The backup structure is a truss frame of carbon-fiber-reinforced plastic rods and invar steel nodes. The surface consists of 60 panels consists of a composite of carbon-fiber-reinforced plastic sheets epoxied to an aluminum honeycomb core. The specified and achieved performance of the HHT are summarized in Table 2. Using holography with a satellite-signal source, the surface could be set to an overall precision of 12 μm rms. This was the best ever reached in the late nineties, and has only recently been repeated for the ALMA antenna of 12 m diameter.

The enclosure is a barn, the roof panels and front doors of which are opened during operation. They provide a reasonable decrease in wind effects on the pointing.

Observations of planets, located near the sun, showed the high quality and stability of the surface and pointing, even when the sun was illuminating part of the reflector [32]. Several new technical methods and solutions were introduced and developed in this project, which paved the way for later sub-millimeter telescopes, such as ALMA, to be described next.

Figure 25. (a) The European ALMA antenna, delivered by consortium AEM. (b) The US antenna, produced by Vertex. In both, the carbon-fiber-reinforced plastic reflector backup structure is shielded against solar radiation by outside cladding. Steel parts of the yoke and base are covered with thermal insulation. The reflector diameter is 12 m and the surface precision is about 20 μm rms (ALMA-ESO/NOAJ/NRAO).

5.3 Atacama Large (Sub-) Millimeter Array (ALMA)

Despite the short wavelength, but restricted by the relatively small reflector size, the best angular resolution of mm-telescopes remained of the order of 10 arcseconds. To achieve better than one-arcsecond resolution, interferometers for the mm-domain were realized in the years 1985 to 1995 in France (IRAM), Japan (Nobeyama), and the USA (OVRO, Caltech and BIMA, Berkeley, Illinois/Maryland). These arrays consisted of three to 10 antennas of 6 m to 15 m diameter, with baselines up to 500 m. In the mid-1990s, proposals for much larger and more-sensitive arrays were being independently developed in the USA, Japan, and Europe. The concepts entailed up to 50 antennas of 8 m to 15 m diameter, to be spread over up to ten kilometers of baseline. All three groups identified the altiplano at 5000 m altitude near the 6000 m high Chajnantor Mountain in the northern Atacama Desert of Chile as the best site for the array. The atmospheric quality of this site would enable observations in all atmospheric windows up to 1 THz, and the flat terrain allowed for the envisaged baselines of more than 10 km. The three proposals differed quite substantially in the layout of the array, based on different priorities of astrophysical research.

From 1997 onwards, plans were discussed to combine the three separate array proposals into one large, global Millimeter Array, actually working in the sub-millimeter domain up to 1 THz. In 2002, this led to the formation of ALMA, the *Atacama Large Millimeter Array*, with major partners North America (USA and Canada) and Europe (many countries, coordinated by ESO), each contributing 50 percent of the *basic instrument*, and East Asia (Japan, Taiwan, and Korea) as a third partner, with a smaller contribution for so-called *enhancements*. It was by far the largest project in astronomy, undertaken in a global collaboration to build an instrument of truly magnificent performance: at least an order-of-magnitude better in sensitivity, angular resolution, and spectral coverage than any existing millimeter telescope.

Table 3. The specifications of the ALMA antennas under operational conditions.

Reflector diameter	12 m
Reflector accuracy*	25 μm – goal 20 μm
Absolute pointing	2" over all sky
Offset pointing	0.6" over 2° radius (w.r.t. calibrator source)
Fast pointing switching	1.5° move in 1.5 s, settle to 3" peak error
Path length stability	15/20 μm (non repeatable/repeatable)

Operating conditions: temperature: –20 °C to +20 °C, $\Delta T_{amb} < 0.6 / 1.8$ °C in 10/30 minutes
full solar loading, including solar observation
average wind velocity: < 6/9 m/s for day/night, respectively

*includes main and subreflector, fabrication, gravity, wind and thermal deformation

ALMA consists of the basic *synthesis array* of 50 antennas of 12 m diameter, equipped with a cryogenically cooled system containing 10 separate receiver cartridges covering the frequency region from 30 GHz to 950 GHz (excluding the atmospheric absorption bands). The enhancement consists of a set of four 12-m antennas plus a *compact array* of a dozen 7-m antennas for the measurement of the total intensity of extended objects and coverage of the shortest baselines below the minimum separation between the 12-m antennas needed to avoid collision and excessive shadowing [33]. The array occupies a large, remarkably flat area at about 5000 m altitude in the Atacama Desert in northern Chile. The extremely dry atmosphere above the site allows sensitive observations up to about 1 THz. The specifications of the antennas were consequently tailored to this goal, as illustrated in Table 3.

Dedicated single sub-mm telescopes have normally been protected against the major influences of the environment by an enclosure. The telescope itself thus could be optimized for operation under the relatively benign operational conditions, without the need to accommodate survival loads. In the case of the multi-element ALMA telescope, a protective dome was out of the question. The main reason was that the antennas would be moved between stations over distances of more than 10 km. A dome-protected and transportable antenna was not economically viable. As a result, the ALMA antenna design had to not only obey the stringent performance specifications, but the structure also had to be able to withstand rather extreme survival loads without damage.

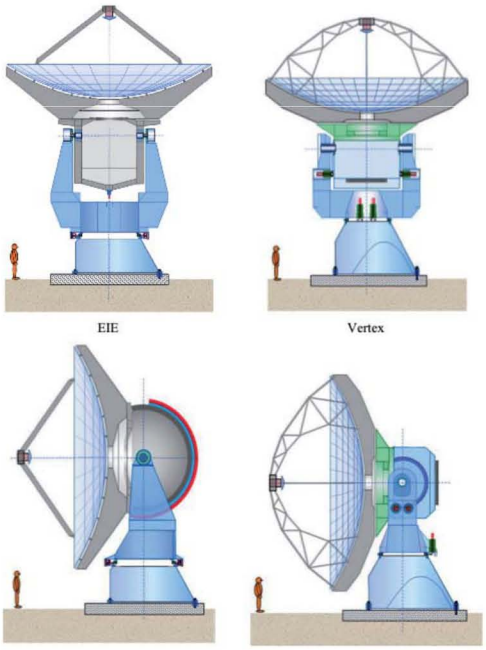

Figure 26. A color-coded comparison between the AEM/EIE and Vertex antennas: Grey = carbon fiber composite; green = INVAR; blue = steel; red = drives/magnets.

The ALMA project started with the acquisition of two prototype antennas of 12 m diameter. Vertex designed and delivered one to NRAO, and a consortium of Alcatel/EIE/MAN delivered another to ESO. Both antennas, placed side by side, were subjected to an intensive test program [34]. Both antennas were acceptable in view of the specifications. In a protracted bidding process, it transpired that each partner would acquire 25 antennas. Vertex delivered to NRAO/AUI, and ESO acquired 25 antennas from the Consortium Thales/Alenia Space – European Industrial Engineering (EIE) – MT Mechatronics, which we denote by AEM. Each company manufactured to their own design. A picture of both antenna types is shown in Figure 25.

The layouts of the two designs are sketched in Figure 26. The foundation ring and the yoke-shaped alidade of the European (AEM) antenna are made of steel, covered by a layer of thermal insulation. The entire structure rotating about the elevation axis (the elevation cradle with incorporated receiver cabin, reflector backup structure, and quadripod) were realized in carbon-fiber-reinforced plastic. Special attention was given to the isostatic decoupling between the two major sections, made of different materials. We give some details of this feature below. The AEM antenna employs symmetrically arranged direct-driving torque motors, thereby avoiding any backlash and reaction forces on the bearing. The quadripod is a single, straight, carbon-fiber-reinforced plastic tube that attaches at the rim of the reflector. This avoids spherical-wave aperture blocking. The reflector consists of 120 panels of about one square meter in area, arranged in five concentric rings. They are made of electroformed nickel front and back skins, with an aluminum honeycomb sandwich core, developed and manufactured by the company Media Lario, in Italy.

The Vertex antenna also has its foundation ring and alidade made in steel, covered by thermal insulation. The receiver cabin and elevation structure are also of steel. A transition cone of invar steel makes the connection to the

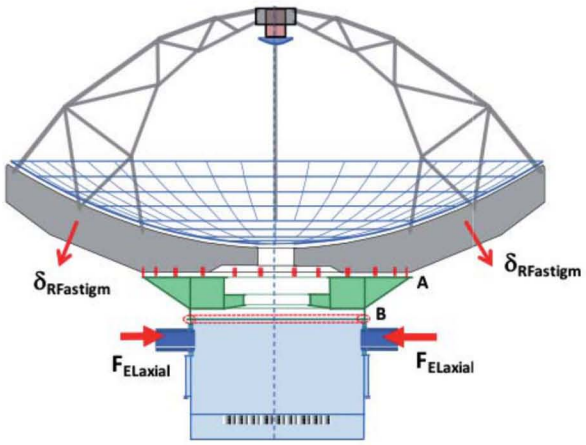

Figure 27. An illustration of the astigmatism of the Vertex antenna under the temperature difference between the yoke-type alidade and the receiver cabin, annex reflector backup structure.

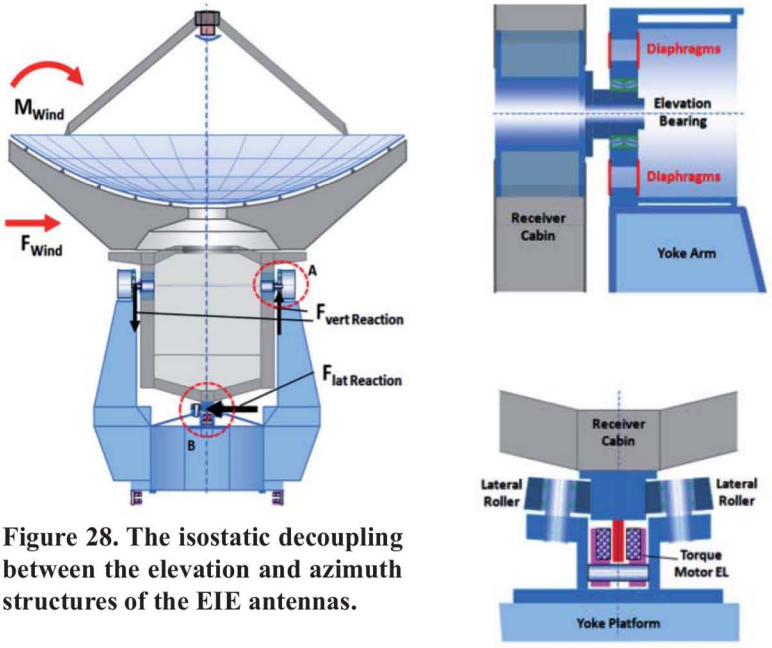

Figure 28. The isostatic decoupling between the elevation and azimuth structures of the EIE antennas.

carbon-fiber-reinforced plastic reflector backup structure through a set of flexures, similar to the solution for the HHT, as described above. The backup structure is a composite of carbon-fiber-reinforced plastic skins, bonded to an aluminum core. The drive system is a conventional geared drive, with standard servomotors at high rated speed that is reduced to antenna speed by a planetary gear train. The Vertex quadripod shows a complicated curved truss system with the aim of minimizing spherical blocking. The total geometrical blocking of the two antennas (4%) is actually essentially the same. The Vertex antenna employs 264 reflector panels arranged in eight rings. They are machined aluminum panels with a size of about a half square meter, the relatively small size being dictated by the maximum range of the high-precision milling machine.

The arrangement of circular blades between the backup structure and the elevation cradle is often used for structures made of materials with different thermal elongation coefficients. The influence of a uniform expansion or shrinking of the backup structure is compensated for by the flexibility of the blades. However, the decoupling by the blades is not total: other types of disturbances in the elevation cradle can still protrude to the reflector and distort its shape.

After commissioning, the US antennas showed a degradation of the reflector accuracy above the specified values near the end of the operational temperature range. This could be explained with reference to Figure 27. A temperature difference between the yoke-type alidade and the receiver cabin activates axial reaction forces in the elevation bearings that distorts the cabin walls. These distortions have no circular symmetry as the distortions by uniform temperature differences for which the circular blades are designed, but can protrude through the Invar structure to the backup structure and result in the indicated astigmatic deformation. The remedy would be an active removal of temperature differences between the receiver cabin and the yoke alidade.

Because of the exposed location of the antennas at the high site, the influence of wind on the pointing stability is of special concern. The requirement is less than one arcsecond fluctuation in a 9 m/s wind with added gusts. A novel approach to this problem was realized by EIE in the European antenna by isostatic decoupling of the elevation and alidade sections (Figure 28). The horizontal wind forces are not directly transferred to axial forces in the elevation bearings, as normally done in other antennas and also in the US ALMA antennas. They are transferred to the alidade in the center of the yoke by lateral rollers in the vicinity of the torque motors (Figure 28, lower right). The elevation bearings are completely decoupled from axial loads by diaphragms between their housings and the yoke arms

Figure 29. About one-third of the ALMA array at 5000 m altitude on the Llano de Chajnantor in the Atacama Desert of northern Chile. The main instrument consists of 50 antennas of 12 m diameter and is supplemented by the Atacama Compact Array (ACA) of 12 antennas of 7 m diameter (in the right background of the picture), plus four more 12 m antennas (ALMA-ESO/NAOJ/NRAO, C. Padilla).

Figure 30. The 64-m diameter Sardinia Radio Telescope (SRT) (INAF).

(Figure 28, upper-right sketch). As a consequence, this concept has the tilting moment of the wind forces taken by additional reaction forces at the elevation bearings in the up and downward directions (Figure 28, left sketch). We do not know other antennas with such a system. It appears to work as intended, and does not show the insufficiencies inherent to the circular-blade approach of the US antennas.

In the fall of 2014, all 66 antennas of ALMA, equipped with the extensive receiver system, had arrived at the operations site at 5000 m altitude on the Llano de Chajnantor (Figure 29). Observations with the partially completed array started in 2008. The performance of the antennas was summarized by Mangum [35] for the North American antennas from Vertex, and by Laing [36] for the European antennas from AEM. In the sub-millimeter region, ALMA eclipses anything available at present, whereby the atmospheric quality at the high site adds significantly to the operational efficiency. The antennas perform almost entirely to specification.

ALMA is currently in its fifth observing cycle with an essentially complete operational system. Observations have produced stunning results (almaobservatory.org). The instrument is more than an order of magnitude more powerful than existing millimeter telescopes, both in sensitivity and angular resolution. Baselines up to 15 km have been used, providing angular resolutions of 0.02 arcsecond, better than the Hubble Space Telescope.

6. Sardinia Radio Telescope (SRT)

The history and the scientific goals of the Sardinia Radio Telescope are described in this Special Section of the *Radio Science Bulletin* by N. D'Amico, and a general description with results of commissioning was presented by Bolli et al. [36]. Here, we limit ourselves to a discussion of some technical aspects of the telescope's design.

The Sardinia Radio Telescope, shown in Figure 30, was specified for frequencies up to 100 GHz, and with a goal for the surface accuracy of 150 μm rms. It is equipped with a large suite of primary and secondary receivers. The prime focus receivers are arranged on a rocking bridge in front of the Gregorian secondary, and the Gregorian focus receivers are hosted in a large receiver cabin in the apex area of the main reflector. The receiver exchange is remotely controlled without human interaction on the telescope.

The design concept of the telescope (Figure 31) was developed in a preliminary design phase by US engineers. The "kinked" alidade somewhat resembles the design of NASA/JPL deep-space antennas, and the elevation cradle somewhat resembles the "Effelsberg umbrella" (Figure 5). In the detailed design phase, executed by MT Mechatronics, some strength and deformation issues of the preliminary design were identified, and they provided some exemplary

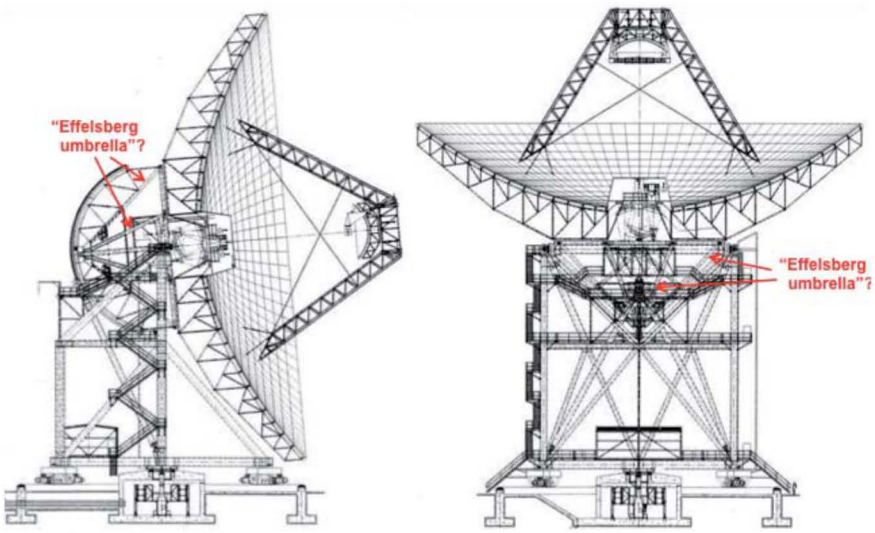

Figure 31. The structural design of the 64 m Sardinia Radio Telescope SRT, as developed in the preliminary design phase.

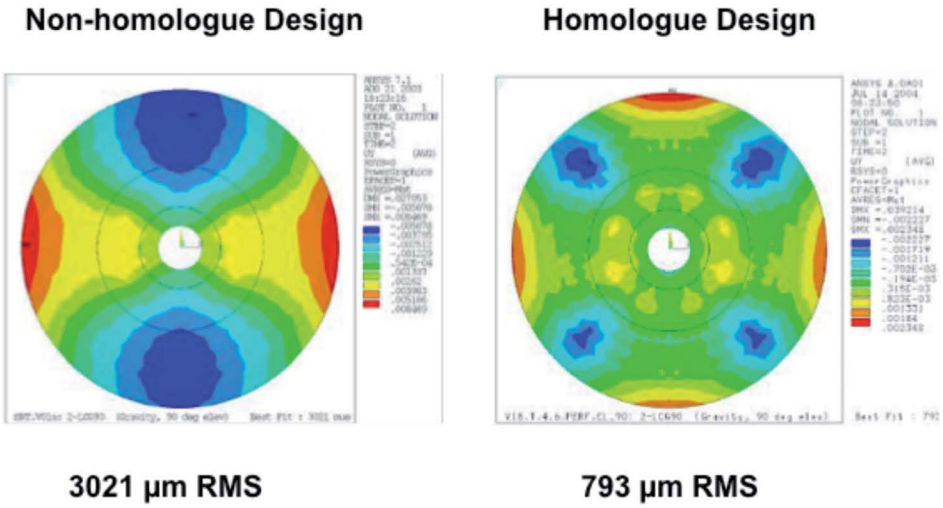

Figure 32. Gravity deformations in the zenith position before (left) and after (right) optimization of the structural concept of the elevation cradle. Note the improvement of almost a factor of four.

insight into the relevance of homology for large radio reflectors.

The finite-element calculation of the reflector's deformations of the preliminary design showed a huge astigmatic deformation pattern in the zenith position (Figure 32, left), which indicated deficiencies in homology, despite the introduction of the "umbrella" concept. They are caused by the inefficient separation of the elevation cradle and backup structure, which we explain below.

The astigmatism was completely eliminated by changes in the load transfer, separating the elevation cradle from the umbrella struts by "flexures." The rms value of the remaining deformations (Figure 32, right) is nearly a factor of four better than that of the preliminary design, and the remaining deformations are dominated by the print-through of the quadripod legs. A further improvement of the homology would need the separation of the quadripod from the backup structure, as in the Effelsberg design, but this was not followed up in this case. The remaining deformations can be compensated for by adjustments of the panels of the active surface.

Details of the preliminary design (Figure 33) showed that four of the eight interface points of the backup structure were interconnected by so-called V-beams (colored pink in the figure), which attract the forces and transfer the loads on the elevation bearings to only four of the eight umbrella points. This causes the astigmatic component in the deformation pattern.

This astigmatic effect was remedied by the introduction of "flexures" instead of the very rigid V-beams (Figure 34, left). The flexures prevent the print-through of the loads of the elevation bearings to the backup structure by their lateral flexibility. In the horizontal position (Figure 34, right), the offset between the location of the elevation axis and the plane of the eight interface points, where the weights of the backup structure are transferred to the umbrella cone, are compensated for by additional "transfer struts." Details of this rather complex structural layout can be identified in the "as built" picture in Figure 35.

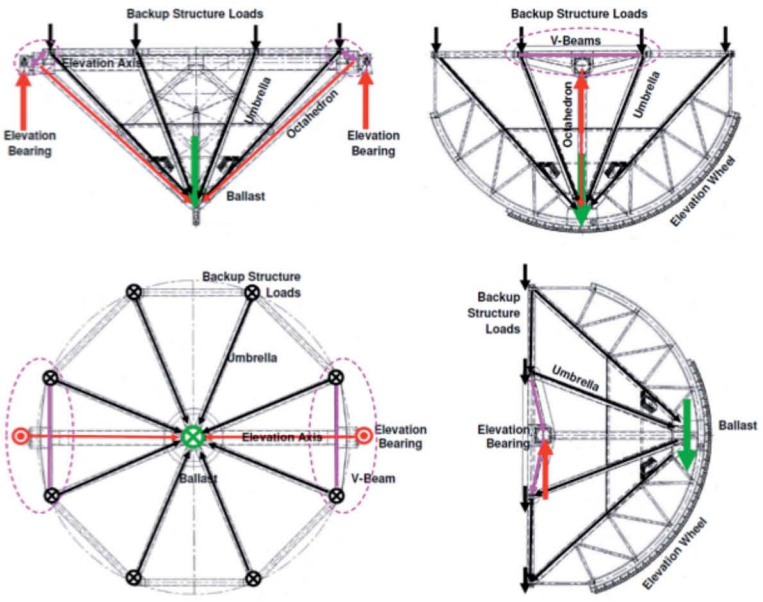

Figure 33. Load paths in the elevation cradle of the SRT with a non-homologous design.

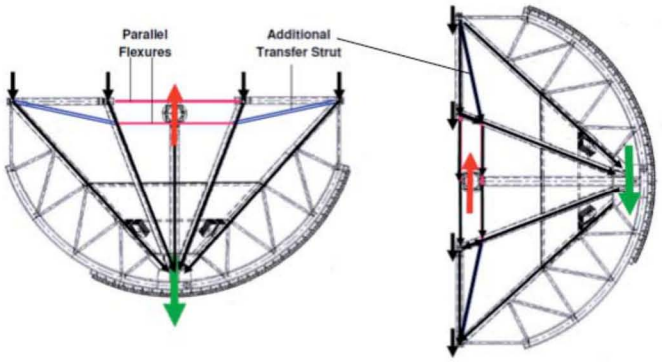

Figure 34. Load paths in the elevation cradle of the SRT with the parallel flexures (pink) and transfer struts (blue), leading to homologous behavior.

The diagram in Figure 36 illustrates the advantages of homologous design in regard to overall reflector accuracy. It assumes the perfect adjustment of the reflector surface at an elevation position of 45°. The gravity deformations of the preliminary design (red line, "given") are in the two end positions significantly above 1 mm. Increasing the stiffness of some of the struts by enlarging their wall thickness (blue line) did not help. This actually increased the astigmatic deformations and the related rms values. Only the homologous design (black line) in the end positions reached values below 1 mm.

One could argue that all the efforts would not be necessary because they could be compensated for by the active surface. However, this is not fully true, because the missing homology increases the required stroke of the surface actuators, and thereby also decreases their positioning accuracy.

Without going into detail, another disadvantage of the non-homologous design is the concentration of stress in the elevation-bearing area, and the related fatigue problems for the structure. These are among the most critical areas of the design of radio-telescope structures. We note that these fatigue-relevant stresses are also reduced by the "equal softness" approach of homology.

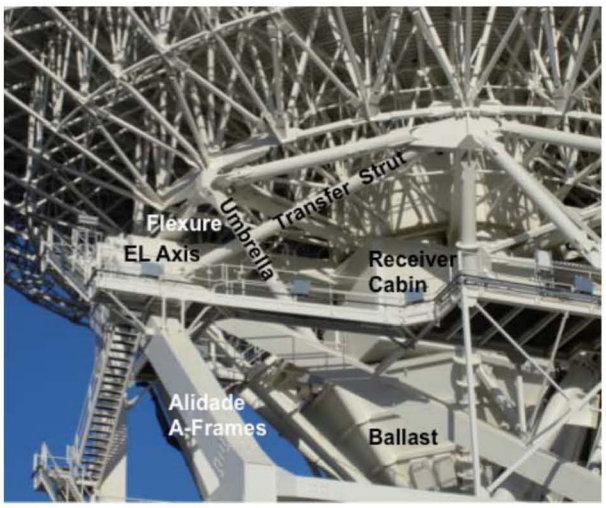

Figure 35. The details of the load transfer to the elevation bearings at the SRT. Note the identification of the essential structural parts in the picture.

7. Conclusion

Among the natural sciences, astronomy holds the unique position of a strictly observational activity. Contrary to the experimental physicist, the astronomer cannot interfere with the conditions of the object under study. He or she is limited to receiving and analyzing the electromagnetic radiation from the object that enters the telescope. The experimental astronomer is thus a telescope and detector builder: a task for mechanical, optical, and electronic engineers. Based on existing knowledge and his or her own ideas, the "pure" astronomer provides performance specifications for a new telescope, such as the diameter of the mirror and the definition of the detector.

In optical astronomy, many telescopes of the 20th century were conceived and realized under the direction of the originating astronomers, and these telescopes were named after them during their lifetime. The most famous example is the Hale telescope of 5 m diameter on Mt. Palomar, in California. More recently, large telescopes were designed and built by a large group of astronomers and engineers, and the name of a major donor may be given to the instrument: for instance, the twin Keck telescopes of 10 m diameter on Mauna Kea, Hawaii.

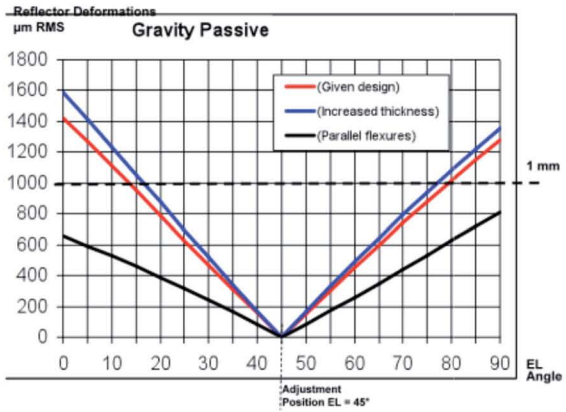

Figure 36. The influence of the homologous design on the amount of gravity deformations a function of elevation.

The emergence of radio astronomy happened along a completely different course. It was essentially an activity by radio and radar engineers, and it took a considerable time until the established optical astronomy community took a serious interest. A notable exception in the early years was astronomer Jan Oort, at Leiden Observatory in the Netherlands, who aimed at deriving the structure of our Galaxy by the observation of the 21 cm spectral line of neutral hydrogen. There are very few radio telescopes that were named after their originators during their lifetime. Only the British radio astronomers Bernard Lovell and Martin Ryle were bestowed with this honor. Jansky had to wait until 2010, when NRAO rechristened the improved VLA to be the Jansky Very Large Array (JVLA).

Once radio astronomy had demonstrated itself as a valuable branch of astronomy, radio observatories were established. Normally, there was a good mixture of astronomers and engineers at those establishments to foster progress in the field. However, in the mid-1960s, the structural engineers encountered the limits of practical and financial possibilities to realistically respond to the requirements of larger reflectors with simultaneously higher surface precision. It is quite interesting to note that a solution to their conundrum was presented by an astronomer/mathematician: the method of *homologous structural design*, conceived by Sebastian von Hoerner [12] showed the way to achieving superior structural performance with much less weight and, hence, cost. The basics of homology, aided by advanced finite-element analysis programs, have enabled the construction of large and highly precise radio telescopes, as illustrated in the foregoing sections.

In this paper, we have presented in broad terms the history of the development of single-reflector radio telescopes by short descriptions of some major examples. A more complete story, together with explanations of the mechanical and structural details of the design of accurate reflector telescopes, has been presented by us in our book, *Radio Telescope Reflectors – Historical Development of Design and Construction* [37], published late in 2017.

We dedicate this paper to the memory of our colleague and friend, Gianni Toffani. He was an astronomer with whom the engineers could have fruitful and engaging discussions. He understood enough of engineering to communicate with engineers and, in the process, to explain to them the astronomical goals and the instrumental requirements for reaching them. In this role, he was instrumental in the successful completion of the beautiful Sardinia Radio Telescope, the third largest in Europe.

8. References

1. K. G. Jansky, "Electrical Disturbances Apparently of Extraterrestrial Origin," *Proc. IRE*, 21, 1933, pp. 1387-1398.

2. G. Reber, "Cosmic Static," *Astrophys.J.*, 91, 1940, pp. 621-624.

3. H. C. van de Hulst, "Radiogolven uit het wereldruim," *Nederlands Tijdchrift voor Natuurkunde*, 11, 1945, pp. 210-221.

4. H. I. Ewen and E. M. Purcell, "Radiation from Galactic Hydrogen at 1420 Mc/s," *Nature*, 168, 1951, p. 356.

5. C. A. Muller and J. H. Oort, "The Interstellar Hydrogen Line at 1420 Mc/s and an Estimate of Galactic Rotation, *Nature*, 168, 1951, pp. 357-358.

6. H. C. van de Hulst et al., "De radiosterrenwacht te Dwingeloo," *de Ingenieur*, 69, 3, 1957, pp. 1-20 (in Dutch).

7. A. C. B. Lovell, "The Jodrell Bank Radio Telescope," *Nature*, 180, 1957, pp. 60-62.

8. E. G. N. Bowen and H. C. Minnett, "The Australian 210-ft Radio Telescope," *Journal Brit. IRE*, 23, 1962, pp. 49-53.

9. J. W. Findlay, "The 300-Foot Radio Telescope at Green Bank, *Sky and Telescope*, 25, February 1963, p. 68.

10. M. M. Small, "The New 140-Foot Radio Telescope," *Sky and Telescope*, 30, November 1965, p. 267.

11. F. J. Lockman, F. D. Ghigo, and D. S. Balse, "But it Was Fun – The First Forty Years of Radio Astronomy at Green Bank," NRAO Publication, 2007.

12. S. von Hoerner, "Design of Large Steerable Antennas," *Astron. J.*, 72, 1967, pp. 35-47.

13. O. Hachenberg, B. H. Grahl, and R. Wielebinski, "The 100-Meter Radio Telescope at Effelsberg, *Proc. IEEE*, **61**, 1973, pp. 1288-1295.

14. J. W. M. Baars and B. G. Hooghoudt, "The Synthesis Radio Telescope at Westerbork. General Layout and Mechanical Aspects," *Astron. Astrophys.*, **31**, 1974, pp. 323-331.

15. R. M. Prestage, K. T. Constantikes, T. R. Hunter, L. J. King, R. J. Lacasse, F. J. Lockman, and R. D. Norrod, "The Green Bank Telescope," *Proc. IEEE*, **97**, 2009, pp. 1382-1390.

16. R. W. Wilson, K. B. Jefferts, and A. A. Penzias, "Carbon Monoxide in the Orion Nebula," *Astrophys. J. Let.*, **161**, 1970, p. L43.

17. M. A. Gordon, *Recollections of Tucson Operations, The mm-Wave Observatory of NRAO*, Berlin, Springer, 2005.

18. J. W. Findlay, "Operating Experience at the National Radio Astronomy Observatory," in "Large Steerable Radio Antennas," *Annals NY Acad. Sci.*, **116**, 1964, pp. 25-40.

19. J. C. Bennett, A. P. Anderson, P. A. McInnes, and A. J. T. Whitaker, "Microwave Holographic Metrology of Large Reflector Antennas," *IEEE Trans. Antennas Propag.*, **AP-24**, 1976, pp. 295-303.

20. J. W. M. Baars, R. Lucas, J. G. Mangum, and J. A. Lopez-Perez, "Near-Field Radio Holography of Large Reflector Antennas," *IEEE Antennas and Propagation Magazine*, **49**, 5, 2007, pp. 24-41.

21. A. Greve and M. Bremer, *Thermal Design and Thermal Behaviour of Radio Telescopes and Their Enclosures*, ASSL 364, Heidelberg, Springer, 2010.

22. P. Brandt and H. Gatzlaff, "Design of the 30-meter Millimeter-Wavelength Radio Telescope," *Technische Mitteilungen Krupp, Forschungsberichte*, **39**, 1981, pp. 111-124 (in German).

23. D. Morris, J. W. M. Baars, H. Hein, H. Steppe, C. Thum, and R. Wohlleben, "Radio-Holographic Reflector Measurement of the 30-m Millimeter Radio Telescope at 22 GHz with a Cosmic Signal Source," *Astron. Astrophys.*, **203**, 1988, pp. 399-406.

24. H. J. Kärcher, "Enhanced Pointing of Telescopes by Smart Structure Concepts Based on Modal Observers," *Proc. SPIE*, **3668**, 1999, pp. 998-1009.

25. A. Greve, M. Bremer, J. Peñalver, P. Raffin, and D. Morris, "Improvement of the IRAM 30-m Telescope from Temperature Measurements and Finite Element Calculations," *IEEE Trans. Ant. Propag.*, **AP-53**, 2005, pp. 851.

26. R. B. Leighton, "A 10-meter Telescope for Millimeter and Sub-Millimeter Astronomy," Tech. Rep. California Institute of Technology, May 1978.

27. D. Woody, D. Vail, and W. Schaal, "Design Parameters and Measured Performance of the Leighton 10.4-m-Diameter Radio Telescopes," *Proc. IEEE*, **82**, 1994, pp. 673-686.

28. J. D. Bregman and J. L. Casse, "A Simulation of the Thermal Behaviour of the UK-NL mm Wave Telescope," *Int. J. Infrared and mm Waves*, **6**, 1985, pp. 25.

29. K. Akabane, "A Large Millimeter Wave Antenna," *Int. J. Infrared & mm Waves*, **4**, 1983, pp. 793-808.

31. S. Guilloteau et 16 alii, "The IRAM Interferometer on Plateau de Bure," *Astron. Astrophys.*, **262**, 1992, pp. 624-633.

31. J. W. M. Baars, R. N. Martin, J. G. Mangum, J.P. McMullin, and W. L. Peters, "The Heinrich Hertz Telescope and the Submillimeter Telescope Observatory," *Publ. Astron. Soc. Pacific*, **111**, 1999, pp. 627-646.

32. A. Wootten and A. R. Thompson, The Atacama Large Millimeter/Submillimeter Array, *Proc. IEEE*, **97**, 2009, pp. 1463-1471.

33. J. G. Mangum, J. W. M. Baars, A. Greve, R. Lucas, R. C. Snel, P. Wallace, and M. Holdaway, "Evaluation of the ALMA Prototype Antennas," *Publ. Astron. Soc. Pacific*, **118**, 2006, pp. 1257-1301.

34. J. G. Mangum, "The Performance of the North American ALMA Antennas, 36th ESA Workshop on Antennas, 2015.

35. R. A. Laing, "The Performance of the European ALMA Antennas," 36th ESA Workshop on Antennas, 2015.

36. P. Bolli et 37 alii, "Sardinia Radio Telescope: General Description, Technical Commissioning and First Light," *Journal of Astronomical Instrumentation*, **4**, 3 & 4, 2015, 1550008 (20 pp.).

37. J. W. M. Baars and H. J. Kärcher, *Radio Telescope Reflectors – Historical Development of Design and Construction*, Astrophysics and Space Science Library 447, Berlin, Springer, 2017.